J Mater Sci (2009) 44:1324–1332
DOI 10.1007/s10853-009-3273-6

Surface modification of magnesium hydroxide and its application in flame retardant polypropylene composites

Xiaolang Chen · Jie Yu · Shaoyun Guo · Shengjun Lu · Zhu Luo · Min He

Received: 21 October 2008 / Accepted: 13 January 2009 / Published online: 7 February 2009

Abstract In this article, titanate and zinc stearate modified superfine magnesium hydroxide [$Mg(OH)_2$] was filled into polypropylene (PP) as a flame retardant (FR). The structure and morphologies of untreated and treated $Mg(OH)_2$ particles were characterized by Fourier transform infrared (FTIR), wide-angle X-ray diffraction (WAXD), and scanning electron microscope (SEM). PP/$Mg(OH)_2$ (1:1) composites were also prepared in co-rotating twin-screw extruder, and the effects of treatment agents on the rheological behavior, mechanical properties, and flame retardancy of PP/$Mg(OH)_2$ composites were studied. The results from FTIR and WAXD show that treatment agents are adsorbed onto the surface of $Mg(OH)_2$ particles. The complex viscosity (η^*) values of the composites decrease with the addition of various treatment agents. Surface treatment agent could significantly improve tensile and impact strength of PP/$Mg(OH)_2$ composites due to its enhanced interfacial adhesion between $Mg(OH)_2$ particles and the PP matrix. According to limiting oxygen index (LOI), titanate treated magnesium hydroxide (MH) greatly enhanced flame retardancy of PP/$Mg(OH)_2$ composites.

X. Chen
Key Laboratory of Advanced Materials Technology Ministry of Education, School of Materials Science and Engineering, Southwest Jiaotong University, Chengdu 610031, China

X. Chen (✉) · J. Yu · S. Lu · Z. Luo · M. He
National Engineering Research Center for Compounding and Modification of Polymer Materials, Materials Eng and Tech Innovation Center of Guizhou, Guiyang 550014, China
e-mail: chenxl612@sina.com.cn

S. Guo
The State Key Laboratory of Polymer Materials Engineering, Polymer Research Institute of Sichuan University, Chengdu 610065, China

Introduction

Polymers have become more widely used in many fields, such as construction, home furnishings, agricultures, and various industrial applications. However, most polymer materials are flammable to various degrees because of containing high carbon and hydrogen contents. Therefore, their poor flame retardancy restricts its practical applications in these fields. As a result, much attention has been paid to the flammability of polymer materials [1–3]. The flammability of polypropylene (PP) materials is also a serious problem. The most commonly used method to control the flammability of materials is the addition of flame retardants (FRs) to the PP matrix, which is blended into PP matrix to improve the flame retardancy. However, halogen containing compounds, alone or in conjunction with antimony trioxide, produce some problems as toxicity of fire retardants, corrosion during melt processing, and emission of smoke and toxic fumes in processing and fires [4, 5]. Therefore, alternative halogen-free flame retardants (HFFRs) such as aluminum hydroxide (ATH), magnesium hydroxide (MH), and expandable graphite (E.G), which are non-toxic and avoid the above-mentioned troubles. All these HFFRs are perhaps the most environmentally friendly FRs since both release just water vapor during combustion, which has attracted great attention of researchers [6–11].

In recent years, inorganic compound MH as a smoking- and toxic-free additive is one of the most extensive replacements for halogen-based flame retardants, and has been frequently used in the HFFR of polymer materials because of its low cost and high-endothermic decomposition temperature. However, the main disadvantages of MH are high loadings of more than 50% by weight to achieve the required flame retardancy and low FR efficiency. Such

high contents, however, deteriorate the mechanical properties of the filled composites due to the poor compatibility between MH particles and the polymer matrix. Therefore, it is very difficult to increase the flame retardancy and keep good mechanical properties of polymers at the same time. To optimize the reinforcing properties of fillers in polymer, it is essential to render the surfaces of the filler and polymer compatible [12–14]. To achieve this, several types of coupling agents, surface coatings, or similar additives are usually used [15–19], and practical systems have been developed for many polymers with common mineral fillers and reinforcements [20]. However, various surface treatments on MH have different effects on the mechanical properties of the PP/MH composites [21–23]. These treatment agents act by modifying the interfacial region between the inorganic filler and the organic polymer to provide an improved bonding between them. The surface modification of the fillers also affects the rheological behaviors of the melt-filled polymer by improving the dispersion of the particles [24, 25] and reducing the melt viscosity by acting as a lubricant or surfactant [26, 27]. The improvement of some properties of the filled PP composites with surface-treated fillers can be due to these effects or even due to modifications in the crystalline fraction of the matrix [28, 29]. Any surface treatment of the fillers may lead to a change of the nucleation of PP, because the filler surface interacts with polymer through catalytic activity and orientation of molecular segments. In this sense, one important function of the filler treatments is to promote alignment of molecular segments of polymer. This significant improvement is attributed to a modification of the polymer deformation mechanism in the vicinity of the filler particles, resulting in localized voiding, manifested as stress whitening.

In our previous study [14] we have shown that the untreated MH deteriorated the mechanical properties of the PP matrix seriously, while silane and silicon oil modification of MH led to a great increase in both mechanical properties (tensile strength and impact strength) and flame retardancy of the PP composites. Moreover, surface treatment caused the change of crystalline behavior and rheological properties [10]. In this present work, titanate and zinc stearate are selected as the interface modifiers between $Mg(OH)_2$ particles and the polymer substrate. The crystal structural characters and the morphology of untreated and treated $Mg(OH)_2$ particles were investigated by Fourier transform infrared (FTIR), wide-angle X-ray diffraction (WAXD) technique, scanning electron microscope (SEM). Moreover, the effects of type of surface modification on the rheological behavior, the mechanical properties, and flame retardancy of PP/MH (100/100) composites were investigated and reported for the first time.

Experimental

Materials

Polypropylene used in this work was a commercial polymer PP–140, supplied by Baling Petrochemical Ltd. (Hunan, China). Magnesium hydroxide, $Mg(OH)_2$, with an average particle size of 2.0–2.5 μm, was provided by Qindao Haida Chemical Ltd. (Shandong, China). Titanate and zinc stearate were supplied by Changzhou Chemicals Co., Ltd. (Jiangsu, China). Antioxidant 1010 is commercial auxiliary from Milan Chemical Ltd. (Nanjing, China).

Preparation of samples

Modification of MH powders was proceeded according to the following steps. The MH powders were dried at 110 °C for 10 h to eliminate possible absorbed water on the surface of the powders. Then MH powders and treatment agent by the recipe were mixed in a high-speed mixer (Type SHR–10A, made in Jiangsu, China) at 100 °C for 30 min. PP (dried at 80 °C for 6 h) and untreated or treated $Mg(OH)_2$ powders were blended in a twin-screw extruder (Type TSE-40A/400-44-22, L/D = 40, made in Nanjing, China). The temperatures from hopper to die at six different zones are 175, 180, 190, 200, 210, and 215 °C, respectively, and the screw speed is 160 rpm. The extrudate was cut into pellets and injection molded (Type J80M3 V, made in China) at 210 °C into various specimens for test and characterization.

Measurements and characterization

FTIR spectroscopy characterization

The FTIR spectra were recorded using a Nicolet MAGNA-IR 750 spectrophotometer. The untreated or treated $Mg(OH)_2$ powders were mixed with KBr powders, and then the mixture was compressed into plates for FTIR analysis.

Crystal structure measurements

The phase structural identification of untreated and treated $Mg(OH)_2$ crystallite was made by WAXD technique, using CuK_α radiation ($\lambda = 1.54\text{Å}$), equipped with computerized data collection and analytical tools. The X-ray source was operated at a voltage of 40 kV and a filament current of 40 mA. Samples were scanned in 2θ ranges from 5 to 75° at a rate of 1°/min.

Morphology

The morphology and structural investigations of $Mg(OH)_2$ powders, the tensile and impact fracture surfaces of the

composites were performed by a scanning electron microscopy (SEM) (Model HitachiX-650, made in Japan). Gold sputter coated samples were examined using a Cambridge Stereoscan 250 with an accelerating voltage of 10 kV.

Rheological behaviors

Rheological measurements were carried out in an Advanced Rheology Expansion System (ARES). An isothermal dynamic frequency sweep was conducted with a disk of 2.0 mm thickness and 25 mm diameter at a frequency range of 10^{-2} to 10^{2} rad s^{-1}, a strain amplitude of 1%, and a temperature of 200 °C.

Mechanical properties

The tensile test of samples was performed at room temperature with a crosshead speed of 50 mm/min on a Material Test instrument (Model WDW-10C, produced in Shanghai, China). The dimensions of specimens were 120 × 10 × 4 mm.

Notched impact test was performed according to the Chinese regulation GB1048 on a drop weight impact tester (Model ZBC-4B, made in Shenzhen, China). The dimensions of specimens were 60 × 10 × 4 mm. The notched depth is 2 mm and notch tip radius is 0.25 mm.

Limiting oxygen index (LOI)

The limiting oxygen index (LOI) value was measured using a LOI instrument (Type JF-3, made by Jiangning Analysis Instrument Factory, Nanjing, China) on sheets 100 × 10 × 4 mm^3 according to the standard oxygen index test ASTM D2863-77. The LOI value is calculated according to the equation given below:

$$\mathrm{LOI} = \frac{[O_2]}{[O_2] + [N_2]} \times 100\%$$

where $[O_2]$ and $[N_2]$ are the concentration of O_2 and N_2, respectively.

Results and discussion

Structural characteristics of $Mg(OH)_2$ particles

Surface treatment agents will greatly affect on the structural and morphological features of the $Mg(OH)_2$ particles. In this article, $Mg(OH)_2$ particles were treated through two different coupling agents, respectively. The evidence for the presence of surface treatment agents adsorbed onto the surface of $Mg(OH)_2$ particles was obtained using FTIR spectroscopy, as shown in Fig. 1. The peaks at 2926.4 and 2854.3 cm^{-1} are ascribed to the asymmetric and symmetric vibration, of aliphatic groups $-CH_2-$, respectively. Moreover, it can be seen from Fig. 1b, c that the relative intensities of peak at 2926.4 cm^{-1} for treated $Mg(OH)_2$ particles is higher than that of untreated $Mg(OH)_2$ particles. It is an adequate support for indicating that the titanate and stearate agents are adsorbed onto the surface of $Mg(OH)_2$ particles [30]. The spectrum has a sharp and intense peak at 3,698 cm^{-1} is attributed to the O–H band stretch in the $Mg(OH)_2$ crystal structure. The absorption peaks in the range of 1,430–1,660 cm^{-1} are attributed to the O–H stretching mode or the CH_2 scissoring mode in the treatment agents. The peak for treated $(OH)_2$ particles at 1642.1 cm^{-1} disappears, whereas the peak at 1443.8 shifts to 1444.9 cm^{-1}. The strong band at around 445.1 cm^{-1} is assigned to the Mg–O stretching vibration in $Mg(OH)_2$.

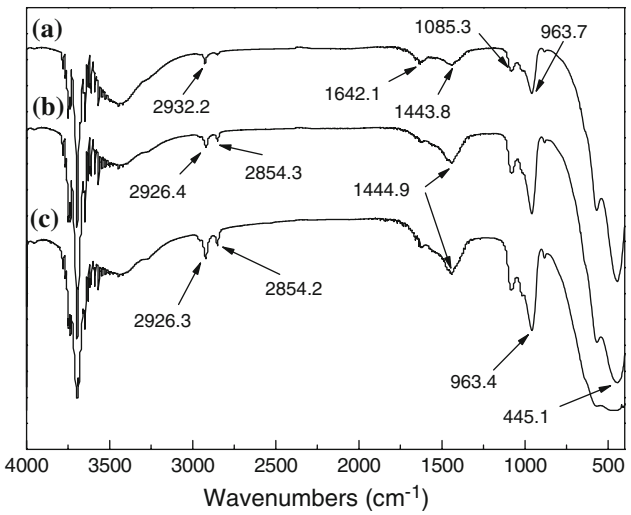

Fig. 1 FTIR spectra of untreated and treated $Mg(OH)_2$: (a) untreated; (b) titanate; and (c) zinc stearate, treated $Mg(OH)_2$ was extracted with acetone for 24 h

The typical powder WAXD patterns of untreated and treated $Mg(OH)_2$ crystals are given in Fig. 2. It can be obviously seen from Fig. 2 that all diffraction peaks can be indexed as the hexagonal structure of $Mg(OH)_2$ with the lattice constants. No WAXD peaks arising from treated $Mg(OH)_2$ particles such as $NaCO_3$ and MgO were detected. Moreover, the intensities of peak at (101) for the treated samples are significantly weaken and narrowed. At the same time, the peak at (100) disappears. All these changes indicate that the grain size of treated $Mg(OH)_2$ particles will have changed, which can be calculated from the WAXD peaks by means of Scherrer formula [31]. As a result, the size of untreated $Mg(OH)_2$ particles of 22.46 nm (001), 37.36 nm (101), 35.79 nm (102), and 39.05 nm (110) in different directions of the crystalline was obtained, whereas the size of corresponding peaks for treated

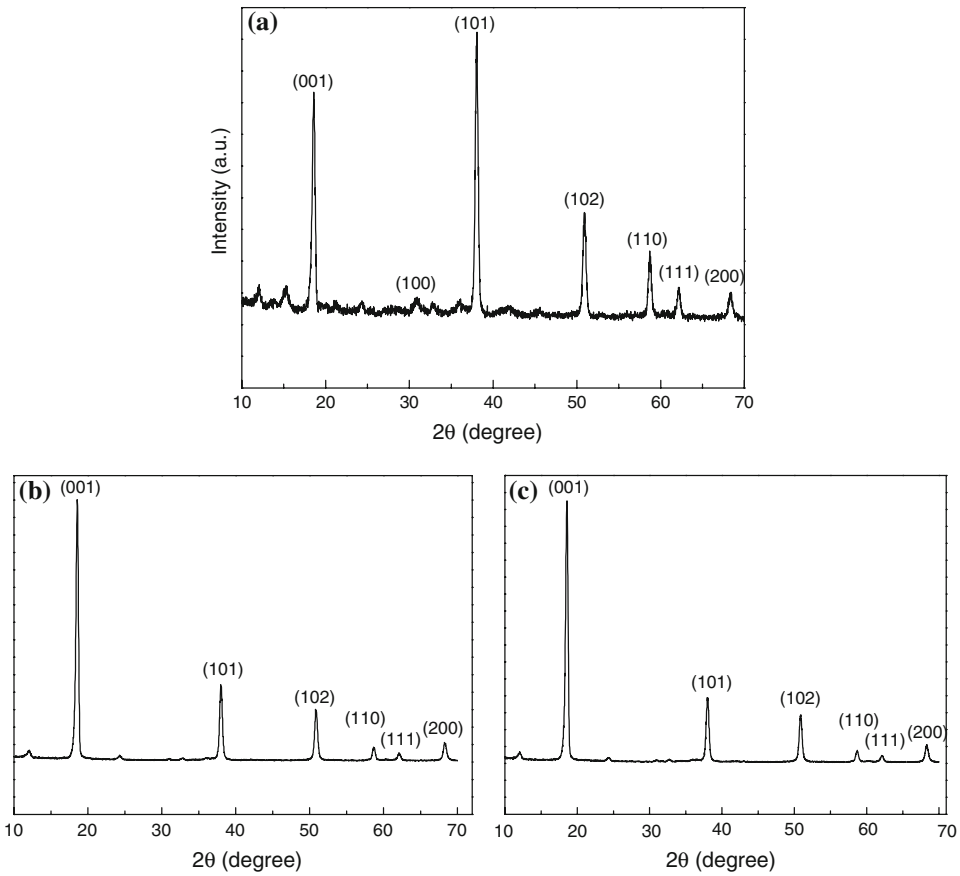

Fig. 2 Powder WAXD pattern of treated $Mg(OH)_2$ particle by various modifiers: **a** untreated; **b** titanate; and **c** zinc stearate

$Mg(OH)_2$ particles have changed due to its different morphology (Tables 1, 2, and 3).

Figure 3 shows the SEM microphotographs of untreated and treated $Mg(OH)_2$ particles. It can be seen from Fig. 3a that there are wide diameter distribution and self-aggregation of $Mg(OH)_2$ particles because of their higher surface energy. And there is hardly single $Mg(OH)_2$ particle, whereas $Mg(OH)_2$ particles are modified by titanate and zinc stearate, respectively, the self-aggregation of the fillers particles disappears, and disperses better. Moreover, the accurate particle diameters can be attained from SEM micrographs. The reason is that surface energy of the

Table 1 Crystallite size of untreated $Mg(OH)_2$ particles obtained from the WAXD pattern (estimated by Scherrer equation)

Diffraction angle 2θ (deg)	Peak position d value (nm)	Miller index (*hkl*)	Crystallite size (nm)	Full width at half-maximum (deg)
18.6	0.7353	001	22.46	0.4544
38.0	0.2365	101	37.36	0.3224
50.9	0.1793	102	35.79	0.3431
58.7	0.1572	110	39.05	0.3308
62.1	0.1493	111	40.92	0.3241
68.3	0.1372	200	25.39	0.4738

Table 2 Crystallite size of titanate treated MH particles obtained from the WAXD pattern (estimated by Scherrer equation)

Diffraction angle 2θ (deg)	Peak position d value (nm)	Miller index (*hkl*)	Crystallite size (nm)	Full width at half-maximum (deg)
18.5	0.4781	001	31.4	0.3537
38.0	0.2367	101	32.0	0.3594
50.8	0.1795	102	32.1	0.3707
58.6	0.1573	110	35.6	0.3529
62.1	0.1494	111	34.8	0.3636
68.2	0.1373	200	32.8	0.3891

Table 3 Crystallite size of zinc stearate treated MH particles obtained from the WAXD pattern (estimated by Scherrer equation)

Diffraction angle 2θ (deg)	Peak position d value (nm)	Miller index (*hkl*)	Crystallite size (nm)	Full width at half-maximum (deg)
18.5	0.4782	001	33.4	0.3386
38.0	0.2367	101	32.0	0.3593
50.8	0.1795	102	30.3	0.3868
58.6	0.1573	110	36.6	0.3461
62.1	0.1494	111	38.5	0.3381
68.2	0.1373	200	29.7	0.4201

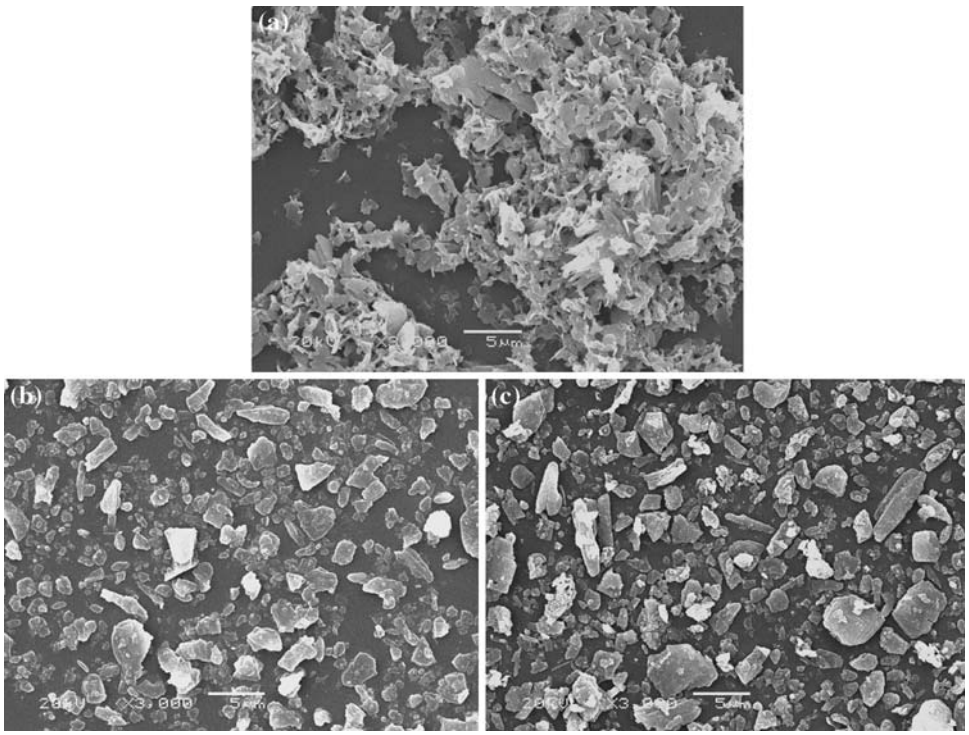

Fig. 3 SEM photos of untreated and treated $Mg(OH)_2$ particles: **a** untreated; **b** titanate; and **c** zinc stearate

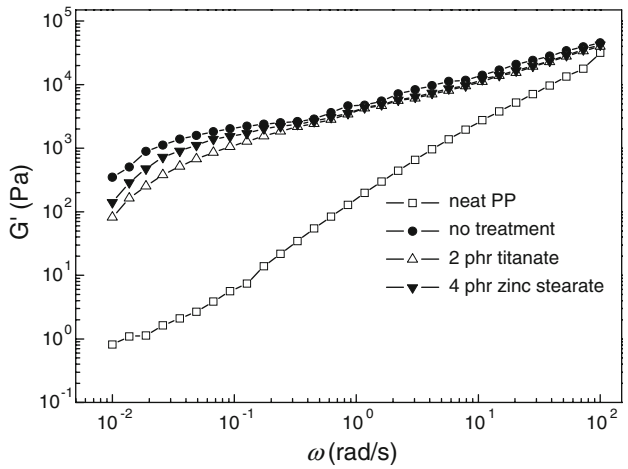

Fig. 4 The relationship of storage modulus (G′) and frequency (ω) for PP and PP/MH(100/100) composites with various surface treatments at 200 °C

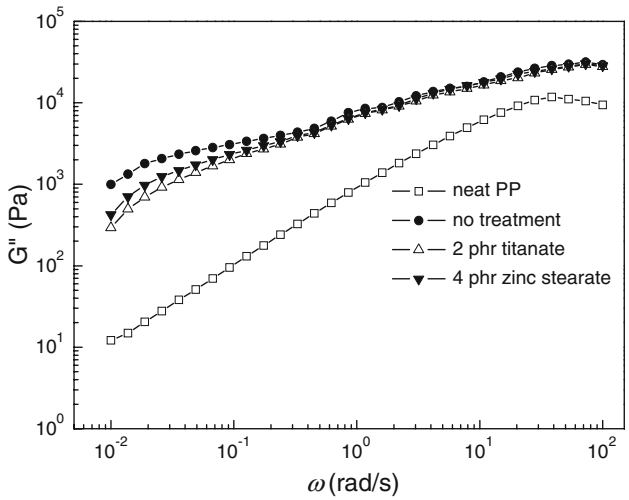

Fig. 5 The relationship of loss modulus (G″) and frequency (ω) for PP and PP/MH(100/100) composites with various surface treatments at 200 °C

treated filler decreases, and thus reduces the effect of filler–filler interaction due to surface treatment is nicely reflected.

Rheological behaviors of PP/$Mg(OH)_2$ composites

The storage (G′) and loss (G″) modulus of PP filled untreated and treated $Mg(OH)_2$ particles as a function of angular frequency (ω) are plotted in Figs. 4 and 5 at 200 °C, respectively. Obviously both modulus increases with increasing ω values. It can be found that the effects are much greater with the compounds than the pure PP matrix. Moreover, the G′ values of each sample are slightly lower than the values of G″. As it is seen, the values of G′ and G″ of the composites with treatment agents are lower than that of the composites without ones, which is more significant at low frequency. The order of both G′ and G″ is consistent with order of no treatment > zinc stearate > titanate > neat PP. This implies that the coupling agents are greater effective on the processing behaviors.

The η^* values of PP/MH composites with various surface treatment agents at 200 °C are shown in Fig. 6.

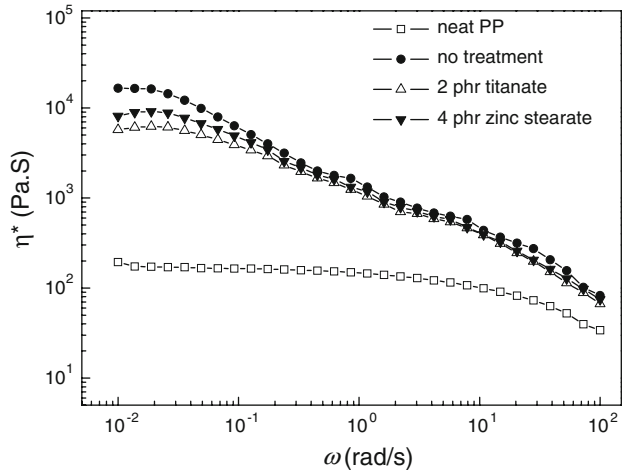

Fig. 6 The relationship of complex viscosity (η^*) and frequency (ω) for PP and PP/MH(100/100) composites with various surface treatments at 200 °C

Obviously neat PP and its composites filled with untreated MH exhibit the typical shear thinning behavior, with a plateau region being observed at low frequency. It can be seen from Fig. 6 that MH has great effect on the η^* of PP at 200 °C, indicating that the difference in η^* of PP and PP/MH composites is very large. Apparently, the PP composites filled with treated $Mg(OH)_2$ particles exhibit a similar behavior to that loading with untreated ones. The η^* values of PP/MH composites with different treatment agents are lower than those of PP/MH composites without modifiers, especially in low-frequency range, confirming that interparticular interactions of $Mg(OH)_2$ particles are reduced as a result of the surface modification. The reason is that surface energy of the treated filler decreases, and thus the treatment agent increases dispersion of primary $Mg(OH)_2$ particles in PP matrix and these well-dispersed $Mg(OH)_2$ particles are responsible for the lower viscosity of the composites. All these can reduce resistance of molecular chains, reducing the viscosities of the composites [32]. Interestingly at high frequency, the η^* values of PP/MH composites did not seem to vary much with and without coupling agents, suggesting no interparticular structure being formed for these treated particles [33].

From the above discussion, it can be concluded that the viscoelastic parameters are improved because of the interaction between the PP matrix and treated fillers. The regid fillers reduced the mobility of PP chains, resulting in increasing the η^* values. However, adding coupling agents improve the dispersion of $Mg(OH)_2$ particles in polymer matrix and reduce the self-aggregation of $Mg(OH)_2$ particles, which has a result in decreasing the complex viscosity, especially at low frequency and when titanate agent is used.

Mechanical properties

In general, the incorporation of FRs causes a decrease in the mechanical properties of polymers [34]. In order to assess the effect of surface modification on mechanical properties of PP/MH(100/100) composites, tensile properties and impact strength were measured. The surface treatment of fillers is the main way for the property improvement of the composites. The effect of modifiers on the tensile properties of PP/MH composites is shown in Fig. 7. The tensile strength and elongation at break of the PP composites with treatment agents are much higher than those of the composites without agents at the same MH loading. The tensile strength of the PP/MH/titanate and PP/MH/zinc stearate composites is about 6–8 MPa higher than that of the PP/MH composites, increasing by ca. 35–45%. This indicates that the addition of coupling agent enhances compatibility between the filler and PP matrix.

Figure 8 presents SEM micrographs of the tensile fracture surfaces for the PP/MH, PP/MH/titanate, and PP/MH/zinc stearate composites. For the composites with untreated MH (Fig. 8a), a very smooth fracture surface can be observed, indicating that the composites is very brittle.

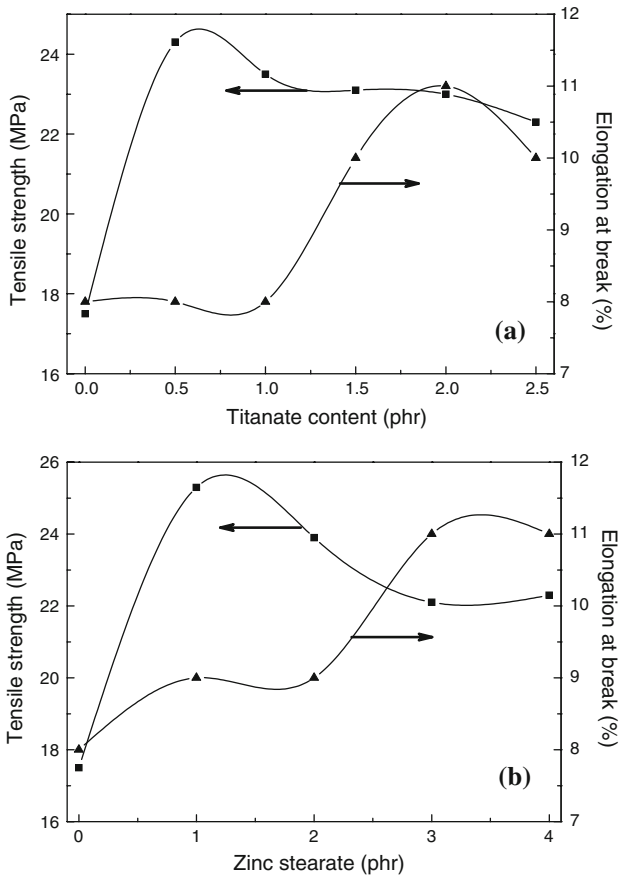

Fig. 7 Effect of the modifiers on tensile properties of PP/MH (100/100) composites: **a** titanate; **b** zinc stearate

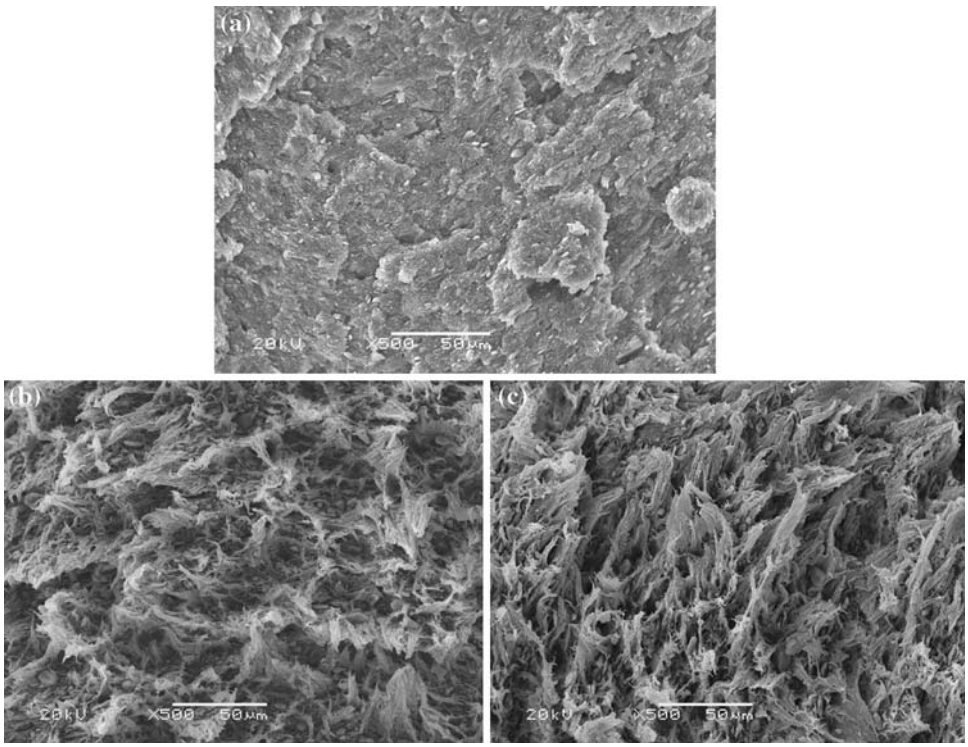

Fig. 8 The tensile fracture surfaces of PP/MH (100/100) composites with and without treatments: **a** no treatment; **b** 2 phr titanate; and **c** 4 phr zinc stearate

However, for the composites with treated MH (Fig. 8b and c), many PP fibrils are observed. These PP fibrils are remnants of the cold-drawn PP ligaments between the rigid $Mg(OH)_2$ particles. Toughening distortion of PP matrix takes place.

The notched impact strength of PP/MH, PP/MH/titanate, and PP/MH/zinc stearate composites is shown in Fig. 9. The impact strength for PP/MH composites is very low. For the PP/MH/titanate composites, the impact strength increases with the increase of titanate content, and passes through a maximum. Then the impact strengths get reduced. However, for PP/MH/zinc stearate composites, the impact strength shows increase trend with increasing zinc stearate content. This indicates that different agent has different effect on the impact strength of the composites.

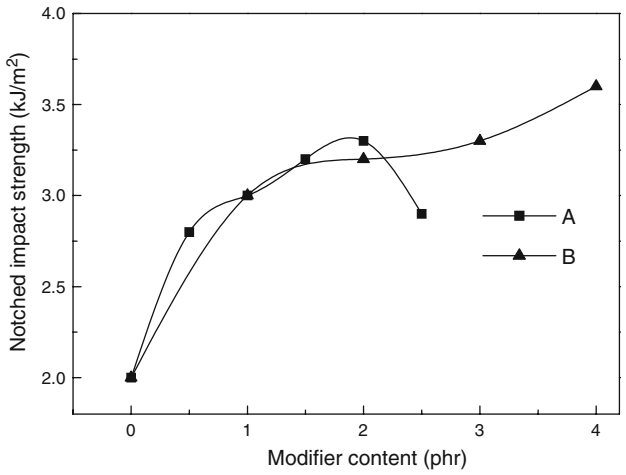

Fig. 9 Effect of the modifiers on impact strength of PP/MH (100/100) composites: (A) titanate; (B) zinc stearate

Figure 10 shows the SEM micrographs of the impact fracture surfaces of PP/MH, PP/MH/titanate, and PP/MH/zinc stearate composites. Compared with untreated MH particles, MH particles treated with modifiers (Fig. 10b and c) become more and more smaller, and MH particles distribution in PP matrix is narrower. Moreover, MH particles are better attached to the PP matrix. It is ascribed to the enhanced interfacial adhesion between the filler and matrix by the surface modification of MH particles, therefore the composites become more ductile.

Flame retardancy

The LOI is widely used to evaluate flame retardancy of polymers [8, 35]. Figure 11 displays the changes of LOI values for the PP/MH composites with different treatment agent content. The result shows that the LOI increases with increasing the content of treatment agent. However, the LOI decreases with further increasing titanate content. These data illustrate that the coating of MH with appropriate content of modifiers greatly improves the flame retardancy of PP/MH composites, especially for titanate treatment agent. The enhancement of FR property may be due to the good dispersion of treated MH particles in PP matrix and the formulation of the compact chars. At the

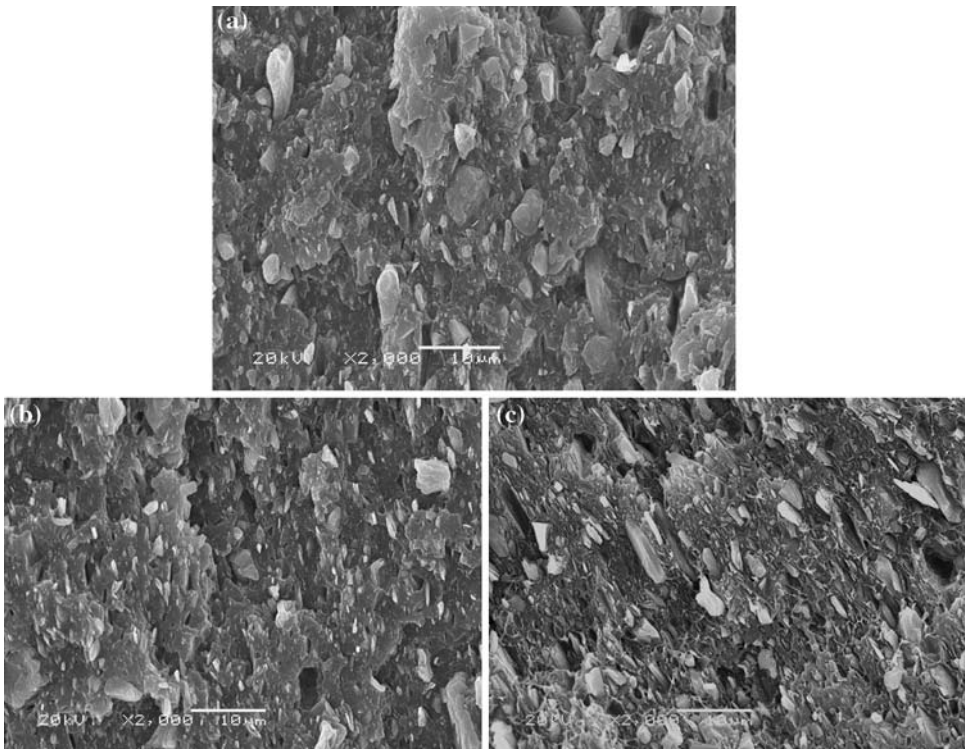

Fig. 10 The impact fractured surfaces of PP/MH (100/100) composites with and without treatments: **a** no treatment; **b** 2 phr titanate; and **c** 4 phr zinc stearate

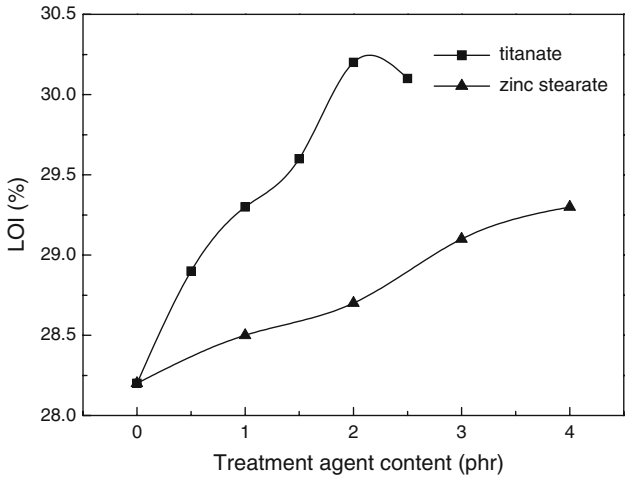

Fig. 11 Effect of surface treatment agents on LOI of PP/MH (100/100) composites

same time, it can be found that the LOI of the composites with titanate higher than that of corresponding composites with zinc stearate.

Conclusions

In this work, $Mg(OH)_2$ particles, as HFFRs, which contains titanate and zinc stearate, have been incorporated into PP matrix. The FTIR result shows that treatment agents molecules are adsorbed onto the surface of $Mg(OH)_2$ particles. The distribution of treated $Mg(OH)_2$ particles is improved better than that of untreated $Mg(OH)_2$ particles. And the self-aggregation of treated $Mg(OH)_2$ particles disappears. The incorporation of $Mg(OH)_2$ increases the values of η^* of PP, whereas treated $Mg(OH)_2$ improves processing behaviors of the PP/MH composites. It is evident that treated $Mg(OH)_2$ greatly improved mechanical properties of PP/MH composites. The SEM analysis shows that the incorporation of treatment agents into the PP/MH composites dramatically enhanced interface adhesion of the composites due to the improvement of the compatibility between $Mg(OH)_2$ and the PP matrix. Moreover, the LOI of PP composites filled treated MH powders could be improved further comparing with the PP/MH composites without treatment agents because of the dispersion of treated $Mg(OH)_2$ particles being enhanced in the polymer matrix.

Acknowledgements The authors are grateful to Science and Technology Foundation of Guizhou province [(2008)7001], Hope Stars Foundation of Southwest Jiaotong University (2008-12), National 863 Project Foundation of China (2003AA32X230), and National Science and Technology Supporting Project Foundation of China (2007BAB08B05) for financial supports of this work.

References

1. Rothon RN (1995) Particulate-filled polymer composites. Longmans, Harlow, NY
2. Chiu S, Wang W (1998) J Appl Polym Sci 67:989

3. Tal CM, Robert K, Li Y (2001) J Polym Sci Part B: Polym Phys 80:2718
4. Warren LM (1988) Plast Technol 34:54
5. Kim S (2003) J Polym Sci, Part B: Polym Phys 41:936
6. Wang ZZ, Wu GS, Hu Y (2002) Polym Degrad Stab 77:427
7. Modesti M, Lorenzetti A, Simioni F et al (2002) Polym Degrad Stab 77:195
8. Chen X, Wu H, Luo Z, Yang B, Guo S, Yu J (2007) Polym Eng Sci 49:1756
9. Chen X, Yu J, Guo S, Luo Z (2008) J Macromol Sci, Part A: Pure and Appl Chem 45:712
10. Chen X, Yu J, Guo S, Luo Z, He M, Polym Compos. doi: 10.1002/pc.20638
11. Chen X, Yu J, He M, Guo S, Luo Z, Lu S, J Polym Res. doi: 10.1007/s10965-008-9236-9
12. Hornsby PR (2004) Fire Mater 18:269
13. Wang ZZ, Qu BJ, Fan WC, Huang P (2001) J Appl Polym Sci 81:206
14. Chen X, Yu J, Guo S (2006) J Appl Polym Sci 102:4943
15. Monte SJ, Sugerman G (1984) Polym Eng Sci 24:1369
16. Cook M, Harper JF (1996) Plast Rubb Proc Appl 25:99
17. Demjen Z, Pukanszky B (1997) Polym Compos 18:741
18. Chuah AW, Leong YC, Gan SN (2000) Eur Polym J 72:313
19. Wang ZZ, Shen XF, Fan WC et al (2002) Polym Int 51:653
20. Griffiths JB (1990) Plast Rubb Process Appl 13:3
21. Hornsby PR, Waston CL (1995) J Mater Sci 30:5437. doi: 10.1007/BF01159314
22. Hornsby PR, Mthupha A (1996) Plast Rubb Proc Appl 25:347
23. Wang J, Tung JF, Fuad MYA et al (1996) J Appl Polym Sci 60:425
24. Han CD, Sandford C, Yoo HJ (1978) Polym Eng Sci 18:849
25. Carpentier F, Bourbigot S, Bras M, Delobel R (2000) Polym Int 49:1216
26. Han CD, Weghe TVD, Shete P, Haw JR (1981) Polym Eng Sci 21:196
27. Jha NK, Misra AC, Bajaj P (1986) Polym Eng Sci 26:332
28. Rybnikar F (1981) J Macromol Sci Phys B 19:1
29. Mitsuishi K, Ueno S, Kodama S et al (1991) J Appl Polym Sci 43:2043
30. Salkar RA, Jeevandam P, Kataby G et al (2000) J Phys Chem B 104:893
31. Cuttity BD (1978) Elements of X-ray diffraction, 2nd edn. Addison-Wesley Publishing Company, Inc., Reading, MA, USA, p 555
32. Hippi U, Mattila J, Korhonen M, Seppälä J (2003) Polymer 44:1193
33. Wang Y, Yu M (2000) J Polym Compos 21:1
34. Kwang JK, James LW, Sang ES et al (2004) J Appl Polym Sci 93:2105
35. Chen X, Yu J, Guo S (2007) J Appl Polym Sci 103:1978